# Terahertz response of dipolar impurities in polar liquids: On anomalous dielectric absorption of protein solutions

Dmitry V. Matyushov*
*Center for Biological Physics, Arizona State University, P.O. Box 871604, Tempe, Arizona 85287-1604, USA*
(Received 23 October 2009; published 12 February 2010)

A theory of radiation absorption by dielectric mixtures is presented. The coarse-grained formulation is based on the wave-vector-dependent correlation functions of molecular dipoles of the host polar liquid and a density structure factor of the solutes. A nonlinear dependence of the dielectric absorption coefficient on the solute concentration is predicted and originates from the mutual polarization of the liquid surrounding the solutes by the collective field of the solute dipoles aligned along the radiation field. The theory is applied to terahertz absorption of hydrated saccharides and proteins. While the theory gives an excellent account of the observations for saccharides, without additional assumptions and fitting parameters, experimental absorption coefficient of protein solutions significantly exceeds theoretical calculations with dipole moment of the bare protein assigned to the solute and shows a peak against the protein concentration. A substantial polarization of protein's hydration shell, resulting in a net dipole moment, is required to explain the disagreement between theory and experiment. When the correlation function of the total dipole moment of the protein with its hydration shell from numerical simulations is used in the analytical model, an absorption peak, qualitatively similar to that seen in experiment, is obtained. The existence and position of the peak are sensitive to the specifics of the protein-protein interactions. Numerical testing of the theory requires the combination of dielectric and small-angle scattering measurements. The calculations confirm that "elastic ferroelectric bag" of water shells observed in previous numerical simulations is required to explain terahertz dielectric measurements.

DOI: 10.1103/PhysRevE.81.021914 PACS number(s): 87.15.H−, 77.22.−d, 61.20.Gy, 61.25.Em

## I. INTRODUCTION

Dielectric spectroscopy of mixtures is a well-established technique which requires theoretical modeling for the data interpretation. The models of dielectric response of mixtures traditionally operate by assuming that a mixture can be separated into macroscopic dielectric bodies. Among the commonly used models are the Maxwell-Wagner theory [1] and various formulations of the effective-medium approximation [2]. Both assume that a dielectric constant can be assigned to each component and the latter also requires that the physical properties of the host and the impurity are not dramatically different.

The recent rapid development of dielectric techniques to study mixtures [3], in particular in the terahertz (THz) frequency window [4], aims at a different length-scale. The interest is mainly driven by the desire to learn about electrostatics of nanoscale objects such as biopolymers [5–11], nanocrystals [12], and nanoconfined fluids [13]. In particular, one hopes that the properties of the nanoscale interface between the solvent and the solute can be effectively probed by the dielectric response. This goal is complicated by the fact that essentially any relaxation event linked to electrical dipoles in the system contributes to the integral experimental signal, and theory is required to separate different components. While a fully atomistic model is the ultimate goal, it is still useful to develop coarse-grained approaches employing the length-scale intermediate between macroscopic dimensions of classical theories [1,2] and a fully atomistic length scale.

This paper presents a coarse-grained model of the dielectric response of dipolar mixtures, aiming in particular at the THz frequency window. The model does not assume that solutes can be described as dielectric bodies, neither does it assume dielectric continuum for a polar solvent. The polar liquid is characterized instead by its wave-vector-dependent correlation functions [14] and a similar approach is invoked for the solutes characterized by their density structure factor. However, instead of using completely atomistic structures, the solutes are modeled by effective spheres specified by dipole moments, polarizabilities, effective radii, etc. The assumption of solute sphericity does not pose a principal restriction on the theory since it can be extended to solutes of nonspherical shapes made by overlapping van der Waals spheres of the composing atoms [15]. However, this simplification allows us to come up with a set of compact analytical equations applicable to analyzing experimental data.

The theory is applied to the analysis of the absorption coefficient of THz radiation. Recent measurements on hydrated saccharides [16] and proteins [17] have shown qualitatively different types of dependencies of THz dielectric absorption on concentrations of these two types of solutes. While the absorption of sacharide solutions decays with increasing solute concentration, the absorption of protein solutions passes through a maximum. The current theory gives an excellent account of the absorption measurements on saccharides but fails to reproduce the protein experiments when the dipole moment of the protein is assigned to the solute. It is suggested that hydrated proteins introduce solvation electrostatics qualitatively different from the dielectric response of typical dipolar mixtures [18]. Specifically, hydration layers nearest to the protein (~10–20 Å in thickness) become polarized and thus carry a significant dipole moment with the

*dmitrym@asu.edu

 

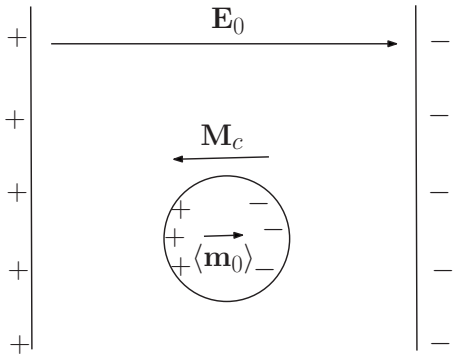


FIG. 1. Schematic diagram of a conventional dielectric impedance experiment. The electric field $\mathbf{E}_0$ (in the absence of dielectric) is perpendicular to the plane of the liquid film such that the field in the dielectric is $\mathbf{E}_0/\epsilon$. This is a longitudinal field as it sets up the direction of symmetry breaking in the homogeneous liquid. The polarization of the cavity in the liquid induces the depolarization field and the corresponding cavity dipole $\mathbf{M}_c$ aligned opposite to the direction of the external field. The average solute dipole $\langle \mathbf{m}_0 \rangle$, aligned along the external field, enhances the dielectric response, but this effect is partially compensated by a concomitant enhancement of the depolarization field of the empty cavity.

relaxation dynamics different from that of the protein [19]. This "elastic ferroelectric bag" [18] surrounding the protein significantly enhances the effective dipole moment of the solute observed on the large wavelength of THz radiation and can account for the observed anomalies in the dielectric absorption of protein solutions [17]. Since both the scenario of the rigid protein dipole and the dipole dressed by the ferroelectric bag of water molecules can be introduced into the formalism, the present theory provides a tool to separate this new physics from what can be described within the traditional understanding of dipolar liquids and solvation electrostatics.

## II. DIELECTRIC RESPONSE OF MIXTURES

We consider a polar liquid with dipolar impurities (solutes). The impurities are larger than the molecules of the host liquid in most cases of practical interest and can physically be realized as molecules or small colloids (nanoparticles). The physics of the problem is clearly presented by separating the process of inserting the impurities into two steps: (i) the creation of a hard-core cavity in the liquid and (ii) polarization of the host polar liquid by the partial charges of the overall neutral solute. The restriction of the solute neutrality can be lifted when ionic conductivity is not an issue such as the case for many THz dielectric measurements.

The creation of a cavity in a polar liquid results, in terms of standard dielectric theories [20,21], in a depolarization field, i.e., charges on the cavity's surface that create the cavity dipole moment $\mathbf{M}_c$ opposite to the direction of the external field. In the standard setup of the dielectric spectroscopy experiment shown in Fig. 1 the electric field is longitudinal, i.e., parallel to the direction of breaking the isotropic symmetry of the liquid by an external perturbation. The dipole of a spherical cavity of volume $\Omega_0$ is then [21] $\mathbf{M}_c = -3\mathbf{P}^L\Omega_0/(2\epsilon+1)$, where $\epsilon$ is the dielectric constant of the homogeneous liquid and $\mathbf{P}^L$ is the longitudinal (superscript "$L$") polarization field created by the external source of the electric field $\mathbf{E}_0$. Since $\mathbf{P}^L = (\epsilon-1)\mathbf{E}_0/(4\pi\epsilon)$, the cavity dipole decreases with increasing $\epsilon$. Standard low-frequency (high $\epsilon$) dielectric measurements of polar liquids are therefore fairly insensitive to impurities.

The dipole moment of the solute orients itself in the external field and therefore enhances the dielectric response. This effect is partially compensated by an additional polarization of the cavity surface by the internal solute dipole acting to enhance the cavity dipole $\mathbf{M}_c$ in the direction opposite to the external field (Fig. 1). The solute dipoles can be considered as independent in the limit of infinite dilution, and the change in the dielectric response is linear in the dipoles' concentration. This approximation limits the range of concentrations by the requirement that the Onsager radius of the solute-solute dipolar interactions is below the average distance between them.

The situation becomes more complex for a finite concentration of solute dipoles when an additional effect of their collective field gains in importance. The alignment of solute dipoles in the external field creates a net average dipole moment $\langle \mathbf{m}_0 \rangle$ (Fig. 1) and a corresponding nonzero net electric field that can potentially polarize cavities and alter their cavity dipoles. Since internal fields are commonly large compared to the external field, this effect, nonlinear in the solutes' concentration, can potentially be significant.

The arguments presented so far apply to the standard dielectric impedance measurements with longitudinal electric fields. THz experiments employ a different geometry where the absorption of a pulse of electromagnetic wave propagating orthogonally to a thin ($\sim$100 $\mu$m) film is measured [6,7]. In this case, the electric field is transversal, i.e., it is perpendicular to the direction of axial symmetry breaking introduced in the isotropic liquid by the direction of the wave vector [22,23]. One measures then the transverse dielectric response and cavities are polarized differently. The dipole moment of a cavity becomes $\mathbf{M}_c^T = -\mathbf{P}^T\Omega_0 \times 3\epsilon/(2\epsilon+1)$, where the transverse polarization (superscript "$T$") is $\mathbf{P}^T = (\epsilon-1)\mathbf{E}_0/(4\pi)$. It is clear that the cavity dipole produced in response to a transversal field is not screened by the high dielectric constant of a polar liquid. Microwave absorption measurements are therefore significantly more sensitive to impurities than conventional dielectric measurements. The distinction between the longitudinal and transverse polarization response in polar substances is the physical basis of the sensitivity of transversal absorption experiments to electrostatics of molecular or nanoscale solutes [4,24].

## III. RESPONSE FUNCTION

We now turn our attention to a detailed analysis of the transverse dielectric response of dipolar mixtures. In order to approach this problem we will use the approximation of linear response of the solvent to the electric field of the solute. The linear response approximation states that the solvent response function is insensitive to the magnitude of the solute electric field and in fact can be calculated for a fictitious

solute with all partial charges turned off (zero dipole for a dipolar solute) [15]. Even though the electrostatic response is linear, the response to the solute repulsive core cannot be calculated within linear models since the repulsive potential produces a large and nonlinear perturbation of the solvent structure. This perturbation renormalizes the spectrum of the solvent fluctuations modifying the linear (Gaussian) response function [25]. In dielectric theories, this modification is included by imposing boundary conditions on the solution of the Poisson equation. The problem becomes way more complex at the molecular level and is commonly solved in terms of angular-dependent distribution functions [26].

We will adopt here Chandler's formulation of the Gaussian model [25] in which the linear response function, modified by the presence of a solute, is sought by imposing the condition of vanishing solvent density from the solute's hard core. In case of the polarization response, this condition implies the polarization field $\mathbf{P}$ vanishing from the hard core of the solute. One can then define a generating functional of the polarization field as follows [14]:

$$\mathcal{G}[\mathbf{E}_0] = \int \exp[-(\beta/2)\mathbf{P} * \boldsymbol{\chi}_s^{-1} * \mathbf{P} + \beta \mathbf{E}_0 * \mathbf{P}] \prod_{i,\Omega_0} \delta[\mathbf{P}(\mathbf{r})] \mathcal{D}\mathbf{P}. \tag{1}$$

Here, $\mathbf{E}_0$ is an external electric field, the asterisk denotes both the volume integration and tensor contraction, and $\beta = 1/(k_B T)$ is the inverse temperature. Further, $\boldsymbol{\chi}_s$ is the two-rank tensor of the Gaussian fluctuations of the polarization field in the homogeneous solvent and the product of delta functions runs over all spatial coordinates $\mathbf{r}$ within solute's hardcore of volume $\Omega_0$ and over all solutes (index $i$). This term ensures that the polarization field vanishes from the volume of each solute in the mixture.

Functional derivatives of $\mathcal{G}[\mathbf{E}_0]$ over the external field $\mathbf{E}_0$ produce correlation functions of the polarization field of the solvent in the presence of the solutes. The Gaussian integral over the polarization field $\mathbf{P}(\mathbf{r})$ can be calculated exactly, resulting in a Gaussian functional in the external field $\mathbf{E}_0$. The corresponding renormalized response function $\boldsymbol{\chi}$ gains most compact representation in the inverted $\mathbf{k}$ space [14]. It can be written in the $\mathbf{k}, \omega$ representation in the following form:

$$\boldsymbol{\chi}(\mathbf{k}_1, \mathbf{k}_2, \omega) = \boldsymbol{\chi}_s(\mathbf{k}_1, \omega) \delta_{\mathbf{k}_1, \mathbf{k}_2} - \sum_i \boldsymbol{\chi}^R(\mathbf{k}_1, \omega) \cdot e^{i(\mathbf{k}_1 - \mathbf{k}_2)\cdot \mathbf{r}_i} \theta_0(\mathbf{k}_1 - \mathbf{k}_2) \cdot \boldsymbol{\chi}_s(\mathbf{k}_2, \omega). \tag{2}$$

Here, $\delta_{\mathbf{k}_1,\mathbf{k}_2} = (2\pi)^3 \delta(\mathbf{k}_1 - \mathbf{k}_2)$ and $\theta_0(\mathbf{k})$ is the Fourier transform of the Heaviside (step) function defining the excluded volume of the solutes considered here as stationary (no translational dynamics). The direct-space Heaviside function $\theta_0(\mathbf{r})$ is equal to unity within the solute and is equal to zero outside the solute. The inverted-space function in Eq. (2) is given by the Fourier integral over the solute volume $\Omega_0$,

$$\theta_0(\mathbf{k}) = \int_{\Omega_0} e^{i\mathbf{k}\cdot\mathbf{r}} d\mathbf{r}. \tag{3}$$

The response function of the mixture $\boldsymbol{\chi}(\mathbf{k}_1, \mathbf{k}_2, \omega)$ depends on two wave vectors $\mathbf{k}_1$ and $\mathbf{k}_2$ separately, instead of $\mathbf{k}_1 - \mathbf{k}_2$ of the homogeneous liquid, because of the inhomogeneous response produced by each solute marked by index $i$. This response function combines the response function of the homogeneous liquid $\boldsymbol{\chi}_s(\mathbf{k}, \omega)$, the information about the solute shape incorporated into $\theta_0(\mathbf{k})$, and the renormalized response function $\boldsymbol{\chi}^R(\mathbf{k}, \omega)$ (see below).

The response function of an axially symmetric dipolar liquid is expandable into longitudinal ($L$) and transverse ($T$) projections [26,27]

$$\boldsymbol{\chi}_s(\mathbf{k}, \omega) = \chi^L(k, \omega)\mathbf{J}^L + \chi^T(k, \omega)\mathbf{J}^T, \tag{4}$$

where $\mathbf{J}^L = \hat{\mathbf{k}}\hat{\mathbf{k}}$ and $\mathbf{J}^T = \mathbf{1} - \hat{\mathbf{k}}\hat{\mathbf{k}}$ are the orthogonal longitudinal and transverse dyads. The $k=0$ values of the response projections are directly related to the frequency-dependent dielectric constant of the host liquid,

$$4\pi\chi_s^L(0, \omega) = 1 - \epsilon(\omega)^{-1},$$

$$4\pi\chi_s^T(0, \omega) = \epsilon(\omega) - 1. \tag{5}$$

The entire $k, \omega$ dependence of the projections $\chi^{L,T}(k, \omega)$ is given in [28], but only the transverse projection is required for the problem considered here (see below).

The last function in Eq. (2) that requires definition is $\boldsymbol{\chi}^R(\mathbf{k}, \omega)$. This function appears in the solution for the generating functional in Eq. (1) as a result of renormalizing the dipolar response of the homogeneous liquid by the solute cavity. It thus contains the information about both the solvent and the solute [14,28]. Only $k=0$ transverse projection of this function appears in the equations for the transverse response of the dipolar mixture to a uniform electric field. It is given by the following equation

$$\chi^{R,T}(0, \omega) = \frac{3\epsilon(\omega)}{2\epsilon(\omega) + 1}. \tag{6}$$

We will now use Eq. (2) to calculate the transverse dipole moment $M^T(\omega)$ of the dielectric sample produced in response to the electric field of the electromagnetic radiation oscillating with frequency $\omega$

$$\mathbf{E}_0(t) = \hat{\mathbf{e}}^T E_0 e^{i\omega t}. \tag{7}$$

Here, the polarization unit vector $\hat{\mathbf{e}}^T$ is perpendicular to the direction of wave propagation $\mathbf{k}$.

The dipole moment $M^T(\omega)$ combines two contributions: the dipole induced directly by the external field of the radiation (radiation wavelength is much larger than any molecular scales in the system) and an additional collective polarization induced by all solute dipoles aligned along the external field. These two contributions are described by correspondingly the first and the second summands in the following relation

$$M^T(\omega) = \hat{\mathbf{e}}^T \cdot \boldsymbol{\chi}(0, 0, \omega) \cdot \hat{\mathbf{e}}^T E_0 + \hat{\mathbf{e}}^T \cdot \boldsymbol{\chi}(0, \mathbf{k}, \omega) * \sum_i \mathbf{T}(\mathbf{k}) e^{i\mathbf{k}\cdot\mathbf{r}_i} \cdot \mathbf{m}_{0,i}(\omega), \tag{8}$$

where $\mathbf{T}(\mathbf{k})$ is the Fourier transform of the dipolar tensor $\mathbf{T} = -\nabla_{\mathbf{r}} \nabla_{\mathbf{r}'} |\mathbf{r} - \mathbf{r}'|^{-1}$ and, as above, the asterisk combines in-

tegration over $\mathbf{k}$ space with tensor contraction. In addition, $\mathbf{m}_{0i}(\omega)$ is the solute's dipole moment aligning along the oscillating external field.

The dipole moment $\mathbf{m}_{0i}(\omega)$ is a sum of two components: the electronic dipole induced instantaneously (on the time scales of interest) by the external filed and a permanent dipole inertially rotated by the torque imposed by the external field. The inertial component can be calculated from the linear response approximation [26] with the result

$$\hat{\mathbf{e}}^T \cdot \mathbf{m}_{0i}(\omega) = (\alpha_{0e} + \alpha_{0n}^T[1 - i\omega\Phi(-\omega)])f_d(\omega)E_0. \quad (9)$$

Here, $\alpha_{0e}$ is the solute electronic polarizability and the permanent (nuclear) dipolar polarizability is given as

$$\alpha_{0n}^T = (\beta m_0^2/2)g_{0,\mathrm{K}}^T. \quad (10)$$

In Eq. (10), $g_{0,\mathrm{K}}^T$ is the transverse Kirkwood factor [29] of the correlated orientations of the solute dipoles

$$g_{0,\mathrm{K}}^T = \left\langle \sum_j [\hat{\mathbf{e}}_i \cdot \hat{\mathbf{e}}_j - (\hat{\mathbf{e}}_i \cdot \hat{\mathbf{k}})(\hat{\mathbf{k}} \cdot \hat{\mathbf{e}}_j)] \right\rangle, \quad (11)$$

and $\hat{\mathbf{e}}_j$ are the unit vectors of the solute dipoles. If dielectric constant $\epsilon_0$ can be assigned to the solutes, then $\epsilon_0 = 1 + 2\pi\beta m_0^2 \rho_0 g_{0,\mathrm{K}}^T$ and $\rho_0 = N_0/V$. We have also assumed isotropic polarizability of the solute and, in addition, for solution problems, the permanent dipole $m_0$ needs to be properly renormalized from the gas-phase value by the effect of the solute polarizability [21,30,31]. Further, the factor $f_d(\omega)$ in Eq. (9) is the Onsager directing field correction [21,30] accounting for the difference between the electric field of the radiation and the local electric field imposing torque on the solute dipole.

The Laplace-Fourier transform $\Phi(\omega)$ in Eq. (9) represents rotational dynamics of the solute dipole

$$\Phi(\omega) = (m_0^2 g_{0,\mathrm{K}}^T)^{-1} \int_0^\infty \hat{\mathbf{e}}^T \cdot \langle \mathbf{m}_0(t)\mathbf{M}_0(0)\rangle \cdot \hat{\mathbf{e}}^T e^{i\omega t} dt, \quad (12)$$

where $\mathbf{M}_0 = \Sigma_j \mathbf{m}_{0,j}$ is the total solute dipole in the sample. In case of a single-time Debye rotational relaxation with the relaxation time $\tau_0$ the term in the square brackets in Eq. (9) gains the form

$$1 - i\omega\Phi(-\omega) = (1 + i\omega\tau_0)^{-1}. \quad (13)$$

The Debye approximation in Eq. (13) is typically sufficient for rigid dipoles dissolved in a polar solvent. The situation potentially becomes more complex for soft nanoscale solutes, biopolymers in the first place. The dynamics of the dipole moment, and the form of $\Phi(-\omega)$, are affected by both the rigid-body rotations and by the low-frequency vibrations of the solute [7]. As we discuss below, the inclusion of a nonvanishing dipole moment of protein's hydration shell, with its own dynamics, makes the problem even more nontrivial, further complicating the form of $\Phi(-\omega)$.

The first term in Eq. (8) can be easily calculated by combining Eqs. (5) and (6) and noting that $\theta_0(0) = \Omega_0$ [Eq. (3)]. This calculation then results in a simple relation for the difference between the response function of the mixture $\chi_{\mathrm{mix}}(\omega) = M^T(\omega)/(VE_0)$ and of the homogeneous liquid $4\pi\chi(\omega) = \epsilon(\omega) - 1$

$$4\pi\Delta\chi = -\eta_0 f(\omega). \quad (14)$$

Here, $\Delta\chi = \chi_{\mathrm{mix}}(\omega) - \chi(\omega)$, $\eta_0 = N_0\Omega_0/V$ is the volume fraction of the solutes in the mixture with the overall volume $V$, and

$$f(\omega) = \frac{3\epsilon(\omega)(\epsilon(\omega) - 1)}{2\epsilon(\omega) + 1}. \quad (15)$$

We note here that a more simple (and elegant) derivation of the response function of a low-concentration mixture as given by Eqs. (14) and (15) can be found in Ref. [20]. Equations (14) and (15) also represent a low-concentration limit of the Maxwell-Wagner formula [1]. Our microscopic consideration is thus consistent with macroscopic arguments. The microscopic description is however required to get correctly the second summand in Eq. (8) describing the collective response of an ensemble of solute dipoles. This is what we consider next.

The response function of the solvent includes two parts corresponding to two summands in Eq. (2). The first summand represents the response of the liquid to an infinitely small solute which does not perturb the spectrum of dipolar fluctuations of the liquid. The contribution of this part of the response function to the transverse dipole moment of the sample [Eq. (8)] is easy to calculate and its relative contribution to the response is $\Delta\chi(\omega)/\chi(\omega) = y_0(\omega)f_d(\omega)$. Here,

$$y_0(\omega) = (4\pi/3)\rho_0\alpha_{0,e} + (2\pi/3)\beta g_{0,\mathrm{K}}^T m_0^2 \rho_0 [1 - i\omega\Phi(-\omega)] \quad (16)$$

is the dipolar density of solutes defined in analogy with a similar quantity of homogeneous liquids [1].

The contribution from the second term in Eq. (2) to $M^T(\omega)$ comes as the correction of the solvent response introduced by the excluded volume of the solute. This calculation is more complex. After some algebra one arrives at the mixture susceptibility relative to the susceptibility of the homogeneous liquid,

$$\Delta\chi(\omega)/\chi(\omega) = -\eta_0 \frac{3\epsilon(\omega)}{2\epsilon(\omega) + 1} + y_0(\omega)f_d(\omega)\left(1 - \frac{3\epsilon(\omega)}{2\epsilon(\omega) + 1} I(\omega, \eta_0, R)\right). \quad (17)$$

The only nontrivial part in this equation is the integral $I(\omega, \eta_0, R)$ arising from the combined effect of the volume excluded by the solute from the solvent, many-body solute-solute correlations, and microscopic correlations between the dipoles of the solvent. All these factors are convoluted into the $k$ integral,

$$I(\omega, \eta_0, R) = \frac{6R}{\pi} \frac{\epsilon(0) - 1}{\epsilon(\omega) - 1} \int_0^\infty dk j_1^2(kR) S_0(k, \eta_0) \frac{\chi_s^T(k, \omega)}{\chi_s^T(0, 0)}, \quad (18)$$

in which $j_1(x)$ is the first-order spherical Bessel function and $R = (\sigma_0 + \sigma)/2$ is the distance of the closest approach of the

solvent molecules with the effective hard-sphere diameter $\sigma$ to the solute characterized by its hard-sphere diameter $\sigma_0$.

The density-density structure factor $S_0(k,\eta_0)$ in Eq. (18) is responsible for a nonlinear dependence of the response function of the mixture on the solute concentration. The $k=0$ value of the structure factor $S_0(0,\eta_0)$ ($S_0(0,\eta_0)\to 1$ at $\eta_0\to 0$) is the reduced compressibility of the solute component of the mixture. It is equal to the experimentally measurable osmotic compressibility [32,33],

$$S_0(0,\eta_0)=\chi_{\rm osm}=\left(\frac{\partial\rho_0}{\partial(\beta\Pi)}\right)_{\rm osm}, \tag{19}$$

where $\Pi$ is the osmotic pressure and the derivative is taken under the condition of osmotic equilibrium.

The transverse dipolar correlation function $\chi_s^T(k,\omega)$ in Eq. (18) does not depend on the solute concentration, but incorporates spacial transverse correlations between dipoles in the polar liquid. We provide its functional form here for completeness and refer the reader to Refs. [28,34] for a more detailed account of this problem

$$\frac{\chi_s^T(0,0)}{\chi_s^T(k,\omega)}=\frac{S^T(k)}{S^T(0)}+\frac{1}{1+p'(k\sigma)^2}\left(\frac{\epsilon(0)-1}{\epsilon(\omega)-1}-1\right). \tag{20}$$

In this equation, $S^T(k)$ is the static structure factor of transverse dipolar fluctuations. A simple extension of the mean-spherical solution for dipolar fluids [27] gives $S^T(k)$ consistent with numerical simulations [34]. This formalism is used here for numerical calculations of the function $I(\omega,\eta_0,R)$ in Eq. (18). Finally, the parameter $p'$ in Eq. (20) quantifies the relative contribution of translational vs rotational motions of liquid's dipoles in the overall response, as discussed in [35].

The approximation of continuous dielectric corresponds to the neglect of the **k** dependence in the transverse response function $\chi_s^T(k,\omega)$ in Eq. (18) assuming $\chi_s^T(k,\omega)\simeq\chi_s^T(0,\omega)$. The dependence on frequency then disappears from the integral $I(\omega,\eta_0,R)$ which simplifies to

$$I(\eta_0,R)=(6R/\pi)\int_0^\infty dk j_1^2(kR)S_0(k,\eta_0). \tag{21}$$

The dielectric-continuum integral $I(\eta_0,R)$ is equal to unity for an ideal solution when $S_0(k,0)=1$. This ideal-solution/continuum limit then results in a simple equation for the mixture's dielectric response,

$$\Delta\chi(\omega)/\chi(\omega)=-\eta_0\frac{3\epsilon(\omega)}{2\epsilon(\omega)+1}-y_0(\omega)f_d(\omega)\frac{\epsilon(\omega)-1}{2\epsilon(\omega)+1}. \tag{22}$$

It shows that the presence of very dilute solute dipoles lowers the transverse response because an enhanced depolarization of the cavity wins over the direct alignment of the solute dipoles along the external field. It is clear that this result cannot sustain itself as the concentration of dipolar impurities grows since the limit of a dielectric constant below unity can potentially be reached. Solution nonideality must slow the negative decay of the mixture susceptibility or reverse its sign to positive.

The continuum integral $I(\eta_0,R)$ in Eq. (18) can be rewritten in **r** space as

$$I(\eta_0,R)=1+(\rho_0/\Omega_0)\int d\mathbf{r}_1 d\mathbf{r}_2 f_0(\mathbf{r}_1)h_0(\mathbf{r}_{12})f_0(\mathbf{r}_2), \tag{23}$$

where $h_0(\mathbf{r}_{12})$, $\mathbf{r}_{12}=\mathbf{r}_2-\mathbf{r}_1$, is the pair correlation function of the solutes and $f_0(\mathbf{r})$ are Mayer $f$ functions representing hard cores of the solutes. If long-ranged interactions between the solutes are neglected, the lowest-order density expansion of the pair correlation function $h_0(\mathbf{r}_{12})$ yields the third virial coefficient $C_{112}$ of the mixture of hard spheres of diameter $R$ (component 1) and diameter $\sigma_0$ (component 2): $I=1-(3\rho_0/\Omega_0)C_{112}$ and $\Omega_0=(4\pi/3)R^3$. The third virial coefficient of the hard-sphere mixture is known [36,37]. For solutes much larger than solvent, one can put $R\simeq\sigma_0/2$ with the result $I(\eta_0)=1-(\eta_0/8)(3+65/24)$. This simple equation compares reasonably well with the direct numerical integration using the Percus-Yevick (PY) expression for the density structure factor $S_0(k,\eta_0)$. The numerical integrals can be approximated by a polynomial of $R/\sigma_0$ and $\eta_0$, and this fit is provided in Appendix for $0\le\eta_0\le 0.3$.

The interactions between hydrated proteins are complex and $S_0(k,\eta_0)$ of a hard-sphere fluid might be a useful approximation only for a limited range of ionic strengths when Coulomb forces are sufficiently screened [38,39]. The structure factor $S_0(k,\eta_0)$ is directly measured by small-angle scattering [39,40] and can be numerically reconstructed from a linear combination of a repulsive and attractive potentials; a combination of Yukawa potentials is often used [40]. The small $k$ part of the structure factor is strongly affected by long-range interactions, and there is a peak at $q_m\simeq 2\pi\sqrt[3]{n_0}$ corresponding to the average distance between the solutes in solution. Since the amplitude of the peak is typically small [39], a general insight into how correlations between hydrated proteins affect the dielectric response can be gained from an empirical approximation for $S_0(k,\eta_0)$. The following approximation (analogous to the empty core model [41]) follows directly from the low-density expansion of the direct correlation function of a hard sphere,

$$S_0(k,\eta_0)=[1+a(\eta_0)j_1(k\sigma_0)/(k\sigma_0)]^{-1}, \tag{24}$$

in which the constant $a(\eta_0)$ is chosen to reproduce the osmotic compressibility $a(\eta_0)=3(S_0(0,\eta_0)^{-1}-1)$. The resulting integral $I(\eta_0,R)$ in Eq. (21) is a function of $a$ only ($R\simeq\sigma_0/2$). Its numerical value can be approximated by a Padé form, $I(a)=(1+0.090\,830\,8a-0.002\,265\,67a^2)/(1+0.131\,266a-0.004\,340\,23a^2)$, which allows one to use the osmotic compressibility, affected by both repulsions and attractions, as input to obtain the dielectric response. The approximation of Eq. (24) is accurate up to $\eta_0\simeq 0.1$ when compared to the direct integration with the PY density structure factor.

It is worth noting at this point that the continuum approximation is inaccurate at low frequencies $\omega\simeq 0$ overestimating the cavity polarization in the entire range of solute sizes of common interest (Fig. 2). This happens because of a very sharp decay of the structure factor $S^T(k)$ at small $k$ values [34] which, in the continuum limit, is replaced by its $k=0$

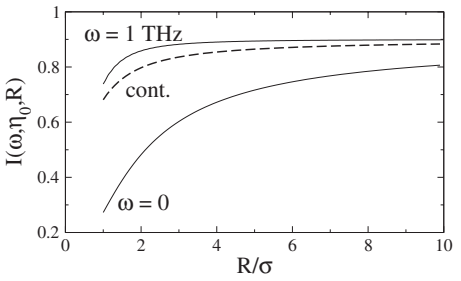


FIG. 2. $I(\omega,\eta_0,R)$ calculated at $\omega=0$ and $\omega=1$ THz as indicated in the plot vs the reduced distance of closest solvent approach to the solute $R/\sigma=(\sigma_0/\sigma+1)/2$. The dashed line is the dielectric-continuum result of Eq. (21); $\eta_0=0.1$ and the solvent parameters are those of water (see Appendix).

value $S^T(0)$. The continuum approximation becomes more accurate as the frequency increases and the dielectric constant drops (Fig. 2), but it needs to be tested before applied in a frequency range of interest. Nevertheless, in the range of THz frequencies, the continuum limit [Eq. (21)] presents a useful simplification of Eq. (18), which, in conjunction with Eq. (24), yields the dielectric response solely in terms of observable quantities.

The actual dependence of the dielectric response on the solute volume fraction is more complex than a nearly linear decay suggested by Eq. (22). It is shown in Fig. 3 where a static $\omega=0$ response is calculated for parameters specific to $\lambda_{5-86}$ protein discussed below. Baxter's solution of the PY closure [26] for $S_0(k,\eta_0)$ was used in these calculations. In addition, the microscopic transverse response function of the solvent dipoles was taken according to Ref. [28], and the static dipolar structure factor was calculated from a corrected mean-spherical approximation suggested in Ref. [34]. The dependence of the dielectric response on $\eta_0$ is curved down, thus eliminating the dielectric catastrophe following from the linear extrapolation of Eq. (22). However, the shape of the concentration dependence varies with the frequency, and the curvature is just the opposite one for the THz response (see below).

A notion regarding theory's approximations is relevant here. One might argue that the point-dipole model is too

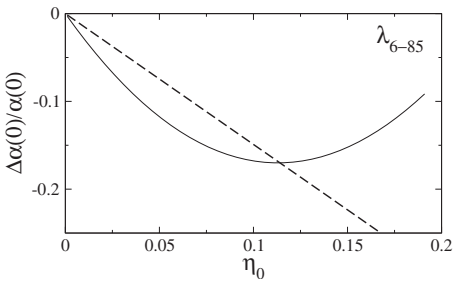


FIG. 3. Relative change in the absorption coefficient of the mixture at $\omega=0$ [see Eqs. (26) and (27)] as a function of the volume fraction of the solute $\eta_0$. The solid line refers to the entire response function from Eq. (17), while the dashed line shows the contribution of the first term only. The latter, linear in $\eta_0$, is the limit of zero solute dipole. The overall nonlinear dependence on $\eta_0$ is the result of mutual polarization of the cavities by the solute dipoles. The solute size and dipole are those of the $\lambda_{6-85}$ protein.

restrictive for the electrostatic field of a protein with a typically nonzero overall charge and the prevalence of charged residues on its surface. We believe that the approximations adopted here are adequate and the theory might actually be more quantitative than it seems. First, the solvent response function is independent of the solute charge in the linear response approximation [34] and is identical to the one obtained for a fictitious solute with all charges turned off. The linear response approximation might obviously fail, and that certainly puts a restriction on the current theory. Second, the perturbation Hamiltonian for the current problem is the interaction of the sample dipole moment with the external electric field of the radiation. Since the THz wavelength obviously exceeds any molecular or nanoscale dimension, the dipolar approximation is appropriate. Finally, the total solute charge can contribute to conductivity [42] that is normally subtracted from the dielectric response and is insignificant in the THz frequency range. The dipole moment of a charged solute is then defined relative to the solute's center of mass [42].

## IV. COMPARISON TO EXPERIMENT

One of the parameters reported in THz dielectric measurements is the relative absorption coefficient $\Delta\alpha(\omega)/\alpha(\omega)$, where $\Delta\alpha(\omega)=\alpha_{\rm mix}(\omega)-\alpha(\omega)$ is the change in the absorption coefficient of the mixture relative to the pure liquid. The absorption coefficient is defined [43,44] as the ratio of the rate of energy dissipation by the medium $\langle\dot{\mathcal{E}}\rangle_\omega$ over the Poynting vector $S(\omega)$ of the incident radiation,

$$\alpha(\omega)=\frac{\langle\dot{\mathcal{E}}\rangle_\omega}{S(\omega)}. \tag{25}$$

By combining the standard equations for the Poynting vector in dielectric media [20,44] with energy dissipation in terms of the dielectric response function $\chi(\omega)$ one gets the equation

$$\alpha(\omega)=\frac{4\pi\omega}{c}\frac{\chi''(\omega)}{\sqrt{\epsilon'(\omega)}}, \tag{26}$$

which can be applied either to the mixture or to the pure liquid ($c$ is the speed of light in vacuum).

Assuming that the deviation of the response $\Delta\chi(\omega)$ caused by impurities is small compared to the dielectric response of the pure liquid, one can easily derive an expression for the relative change of the absorption coefficient,

$$\frac{\Delta\alpha(\omega)}{\alpha(\omega)}=\frac{4\pi\Delta\chi''(\omega)}{\epsilon''(\omega)}-\frac{2\pi\Delta\chi'(\omega)}{\epsilon'(\omega)}. \tag{27}$$

In this equation, the variations in both the imaginary and the real parts of the response are taken into account when impurities are introduced into the polar liquid. In particular, for solutes with small dipole moment, one can drop the term proportional to $y_0(\omega)$ in Eq. (17) and arrive at a simple relation

$$\frac{\Delta\alpha(\omega)}{\alpha(\omega)}=-\eta_0\left[\frac{f''(\omega)}{\epsilon''(\omega)}-\frac{f'(\omega)}{2\epsilon'(\omega)}\right], \tag{28}$$

where $f(\omega)$ is given by Eq. (15).

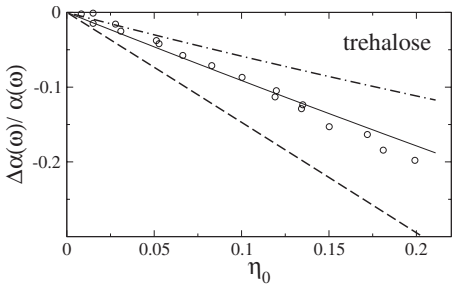


FIG. 4. $\Delta\alpha(\omega)/\alpha(\omega)$ at $\omega=2.5$ THz calculated from Eq. (28) (solid line) and measured experimentally [16] (points) for the aqueous solution of trehalose. The dashed and dash-dotted lines represent, correspondingly, contributions from the first and second terms in Eq. (28) such that the solid line is their difference. The frequency-dependent dielectric constant of water in the THz range of frequencies was taken from Ref. [45] and the molecular volume of trehalose $\Omega_0=278$ Å$^3$ [46] was used to convert from experimentally reported molar concentrations to volume fractions (see Appendix for the details of calculations).

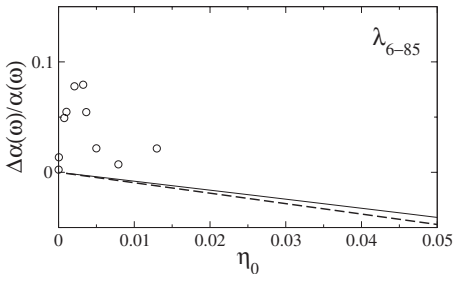


FIG. 5. Relative change in the absorption coefficient at 2.25 THz mimicking the solution of protein $\lambda_{6-85}$ studied by THz spectroscopy in Ref. [17]. The solid line is the dielectric response calculated from Eq. (17) with $m_0=61$ D $(g^T_{0,\mathrm{K}}=2/3)$and the effective radius of 12.1 Å and the points are experimental measurements [17]. The dashed line refers to the first term in Eq. (17) representing the polarization of the solute cavities by the external electric field.

Figure 4 shows the comparison of Eq. (28) (lines) with the experimental absorption coefficients (points) of trehalose dissolved in liquid water [16]. The details of the calculations and the parameters used to produce the plot are given in the Appendix. Because of the small dipole moment of trehalose, a complete calculation of the dielectric response function of the mixture is not required [the term proportional to $y_0(\omega)$ in Eq. (17) is small] and Eq. (28) is sufficient. The dashed and dash-dotted lines in Fig. 4 show the first (imaginary part) and second (real part) terms in Eq. (28). It is clear that changes in the imaginary and real parts of the dielectric susceptibility upon the addition of impurities are comparable in magnitude and should both be included. The only solute parameter entering Eq. (28) is its volume. Equation (28) can therefore be used to determine molecular volumes of weakly polar solutes by means of dielectric measurements.

In an attempt to see what might be the theory prediction for the case of protein solutions we have mimicked the conditions reported in Ref. [17] where the absorbance of the solution of a five helix bundle protein $\lambda_{6-85}$ [47] showed a maximum at the volume fraction of protein below 1% (points in Fig. 5). The calculations (see Appendix for the parameters used) show almost no effect of proteins' dipoles and a negative contribution to the absorption, as in the case of trehalose above and in an obvious disagreement with the experiment.

There is also a clear difference between Figs. 3 and 5. While Fig. 3 shows a clear effect of the mutual cavity polarization by solutes' dipolar fields for the same set of parameters, there is almost no effect of the solute dipolar component in Fig. 5 (cf. solid and dashed lines). The difference comes from the dynamical effect. The solute dipoles do not have time to reorient on the time scale of the THz pulse and the corresponding contribution is strongly diminished by the relaxation $1/(\omega\tau_0)$ term. The THz pulse in this calculation couples almost exclusively to electronic polarizabilities of the hydrated proteins.

For the solute dipoles to be seen in the THz response, either a much faster relaxation or significantly larger effective dipoles are required. Faster relaxation of the protein dipole seems improbable given that numerical simulations show an almost exclusively single-component rotational relaxation with the relaxation time in the range of 3–6 ns [42]. The hydration shell thus emerges as the most probable candidate to explain the differences between the theory and experiment.

In order to obtain more quantitative insights into the problem, results of numerical simulations of protein solutions are required. We found recently [18,19] that, in accord with suggested interpretation of experimental THz data [17], proteins are capable of polarizing their hydration shells $\simeq 10-15$ Å into the bulk water. This polarization results in a significant nonzero average dipole moment of the hydration shell $\langle|\mathbf{m}_w|\rangle$, which reached the value of $\simeq 10^3$ D in simulations of metalloprotein plastocyanin [18]. The dynamics of this ferroelectric cluster around the protein are however decoupled from a much slower tumbling of the protein occurring on the time-scale of nanoseconds. The relaxation of the shell's dipole $\mathbf{m}_w$ is clearly two component. A very fast initial decay, on a subpicosecond time scale, accounts for more than 80% of the relaxation amplitude at 300 K. This fast relaxation correlates with low-frequency vibrations of the protein deforming water's "elastic ferroelectric bag" [19]. The fast component is followed by a low-amplitude tail lasting hundreds of picoseconds. This relaxation component further slows down, but grows in amplitude, with lowering temperature [19].

In the picture of a protein enveloped by the ferroelectric bag of solvation shells the solute dipole $\mathbf{m}_0$ should be replaced by the sum of protein's and shell's dipoles $\mathbf{M}=\mathbf{m}_0+\mathbf{m}_w$. The dynamics of this total dipole provide input to determine function $\Phi(\omega)$, which, together with $\langle M^2\rangle$, yields $y_0(\omega)$ [Eq. (16)]. These parameters were extracted from simulations of plastocyanin carrying the negative charge of −8 in its oxidized state and hydrated by $N_w=21\,076$ TIP3P waters [18,19]. The shell of water molecules of width 20 Å was added to the effective radius of the protein to obtain the effective radius of the protein/water cluster and the volume fraction of coupled protein/water dipoles in solution (see Appendix for details). The dielectric response of the solution was then calculated from Eqs. (17) and (26).

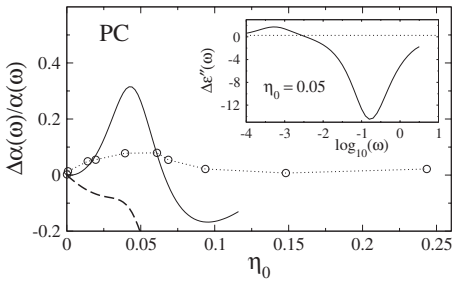


FIG. 6. Change in the absorption coefficient of solution of plastocyanin relative to the bulk water at 2.25 THz. Dipole correlation function of the protein with the surrounding water shell was taken from MD simulations [19]. The solute volume fraction $\eta_0$ was calculated by adding the width of the hydration shell (20 Å) to the radius of plastocyanin (16.8 Å). The points represent the experimental results for $\lambda_{6-85}$ protein [17] recalculated from experimental molar concentrations by using the combined volume of plastocyanin and its polarized water shell. The solid curve refers to the calculations done with the hard-sphere solute-solute structure factor in Eq. (18). In order to show the sensitivity of the results to the solute-solute correlations, the dashed line represents the continuum integral $I(\eta_0)=1-3\eta_0$ with the slope against $\eta_0$ much exceeding that for hard-sphere solutes (long-range repulsions). The inset shows the change in dielectric loss of the plastocyanin solution at $\eta_0=0.05$ relative to the bulk water against frequency measured in $10^{12}$ $s^{-1}$.

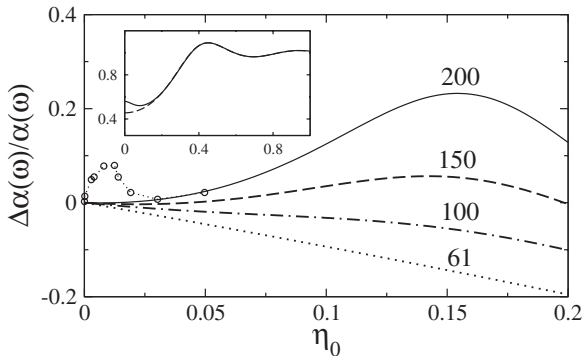


FIG. 7. Change in the absorption coefficient of solution of $\lambda_{6-85}$ protein at 2.25 THz relative to the bulk water. The normalized dipole correlation function of the protein with the surrounding water shell $\Phi(\omega)$ was taken from MD simulations of plastocyanin metalloprotein [19]. The density structure factor of the proteins was constructed from the hard-sphere and Yukawa effective potential [Eq. (29)] obtained in Ref. [49] by fitting small-angle scattering data. The curves refer to different dipole moments (in $D$) of the protein-water cluster as indicated in the plot. The cluster dipoles were assumed uncorrelated, $g_K^T=2/3$. The points are the experimental results from Ref. [17] converted to volume fraction with the hard-sphere diameter $\sigma_0=37.8$ Å from the effective protein-protein interaction potential [49]. The inset shows the density structure factors (vs $k\sigma$) of the Yukawa potential (solid line) and the hard-sphere PY potential (dashed line) at $\eta_0=0.1$.

Figure 6 shows the concentration dependence of the solution absorption coefficient with the PY hard-sphere structure factor $S_0(k,\eta_0)$ (solid line). The points, shown for the reference, are data for $\lambda_{6-85}$ protein [17] rescaled with the volume of the plastocyanin/water cluster. The calculation indeed yields a maximum in the absorption coefficient which turns to negative values with increasing volume fraction. The outcome of these calculations is sensitive to the form of the density structure factor and, therefore, to protein-protein interactions in solution. In order to illustrate this point, the dashed line in Fig. 6 shows the result of calculations with a stronger effect of protein repulsions and thus a steeper decay of $S_0(0,\eta_0)$ with increasing $\eta_0$.

The hard-sphere model might not be adequate for all proteins and electrolyte concentrations. For instance, for the ionic strength employed in Ref. [17] (0.05 M), the interactions between hydrated bovine serum albumin (BSA) proteins are dominated by electrostatic repulsions [48]. These proteins are negatively charged, similarly to plastocyanin, and the long-range interactions are dominated by the screened Coulomb potential. The osmotic compressibility $\chi_{osm}=S_0(0,\eta_0)$ of BSA quickly drops with increasing protein concentration to the level $S_0(0,\eta_0)\simeq 0.1-0.2$ and then does not change significantly when the protein concentration is further increased [48]. With such a dependence of $S_0(0,\eta_0)$ on the volume fraction $\eta_0$ the peak in absorption vanishes (Fig. 6). Note that no absorption peak against protein concentration was detected for BSA in dielectric terahertz measurements at $\omega=1.56$ THz [11].

The inset in Fig. 6 shows the frequency dependence of the dielectric loss $\Delta\epsilon''(\omega)$. As is seen, the change in the loss relative to bulk water can be either positive or negative, depending on the frequency range. A complex concentration dependence seen for the absorption coefficient in Fig. 6 is the cumulative effect of the concentration dependencies of both $\epsilon'_{mix}(\omega)$ and $\epsilon''_{mix}(\omega)$.

The $\lambda_{6-85}$ protein, used to produce Fig. 5, is uncharged. The corresponding protein-protein interaction can be modeled either as a sum of soft repulsion and exponentially decaying attraction or, alternatively, as a sum of hard-sphere ($u_{HS}$) and attractive Yukawa potentials [49],

$$u(r)=u_{HS}(r)-\epsilon(\sigma_0/r)e^{-(r-\sigma_0)/\delta}\theta(r-\sigma_0). \qquad (29)$$

In Fig. 7 we used this latter approximation for the interaction potential to calculate $S_0(k,\eta_0)$ [50] and then applied this structure factor to the calculation of the THz absorption coefficient. In the absence of dipole moment dynamics for this protein, we used the normalized self-correlation function of the protein-water dipole from plastocyanin simulations [18,19]. A set of curves in Fig. 7 refer to different values of the dipole moment of the protein-water cluster, with the lowest curve corresponding to the protein dipole alone (zero shell dipole). Qualitatively, the absorption curves do go through maxima with increasing dipole of the solute and the protein solution absorbs stronger than bulk water. However, the maxima are broader than in experiment and the agreement is only qualitative at best.

The discrepancy between theory and experiment cannot be mended by incremental adjustments to the Yukawa potential in Eq. (29) since the corresponding structure factor is in fact fairly close to that of the PY hard-sphere fluid (inset in Fig. 7). The emergence of the polarization shell around a protein should result in a soft repulsion between hydrated proteins when two shells start to penetrate each other. This

physics is not adequately accommodated by the hard-core repulsion in Eq. (29). A ramp repulsion potential of Jagla type [51] might be a better choice to represent protein spatial correlations in solution. A direct input of $\langle M^2 \rangle$ and $\Phi(-\omega)$ from numerical simulations for the experimentally studied system is also required for a critical test of the theory performance.

## V. DISCUSSION

The present model of the dielectric response targets physical situations when large solutes dissolved in polar solvents do not extend to dimensions of a dielectric material. Large cavities in polar liquids carry depolarization dipoles oriented oppositely to the external field, with their magnitudes scaling linearly with the solute volume. These depolarization dipoles accumulate a negative contribution to the absorption coefficient. The intrinsic solute dipoles, which align along the external electric field, increase the absorption and also produce a nonzero local electric field that repolarizes neighboring cavities. This collective effect, nonlinear in the solute concentration, is sensitive to the solute-solute correlations and is described by convoluting the solvent dipolar response with the density structure factor of the dissolved solutes.

This model performs exceptionally well when tested against experimental THz measurements for weakly polar impurities (Fig. 4). In this case, only depolarization of cavities contributes to the response and that part of the problem seems to be well captured by dielectric theories. Even though solvation of saccharides distorts the structure of water on the microscopic scale [52,53] and slows down the dynamics of the hydration layer [54], THz absorption seems to be insensitive to such changes and the resulting signal is well described by a purely dielectric response. This conclusion is consistent with the recent light scattering spectra of trehalose solutions [54] suggesting only a local perturbation of the water structure restricted to the first solvation shell, which is typical for many small molecular solutes.

Polar impurities introduce both the effect of individual solute dipoles and their collective polarization effect. The response function formalism employed here does not involve any large-scale changes in the solvent structure induced by the solute. This formulation then fails to reproduce the anomalous increase in the absorption of protein solutions over that of bulk water [10,17]. Computer simulations [18] show instead a high extent of cooperativity between hydration shells and protein's vibrations. In addition, a significant polarization of the water shell extending 10–20 Å from the protein surface into the bulk is observed. When the magnitude and correlation function of the protein-water total dipole are substituted into the equations for the solution response, the theory shows a maximum in the absorption coefficient qualitatively similar to experimental observations. The maximum can therefore be considered as an observable signature of the "elastic ferroelectric bag" found by simulations [18]. The shape of this anomalous absorption maximum is however sensitive to the interprotein interaction potential and will be affected by several factors including protein's ionization state and the ionic strength of the solution. All these factors are accumulated in the protein-protein density structure factor available from small-angle scattering measurements. The combination of scattering and THz dielectric data then allows a direct access to the dipole moment dynamics of the protein/water interface, which can be extracted from experiment by using the current model.

## ACKNOWLEDGMENTS

This research was supported by the National Science Foundation (Grant No. CHE-0910905) and TeraGrid CPU allocation (MCB080071). The author is grateful to David Leitner for sharing the simulation results on the lambda repressor protein and to David LeBard for his help with the plastocyanin data.

## APPENDIX: DETAILS OF CALCULATIONS

The dependence of the absorption coefficient on frequency arises predominantly from the frequency-dependent dielectric constant of the solvent. Dielectric measurements of water [45] in the THz range, extended to more typical low-frequency dielectric values, have been used to produce Figs. 2 and 4–7. The dielectric constant is given by the following relation [45]:

$$\epsilon(\omega) = \frac{\Delta\epsilon_1}{1 - i\omega\tau_1} + \frac{\Delta\epsilon_2}{1 - i\omega\tau_2} + \frac{A_S}{\omega_s^2 - \omega^2 - i\omega\gamma_s} + \epsilon_\infty, \tag{A1}$$

where $\Delta\epsilon_1 = 73.9$, $\Delta\epsilon_2 = 1.56$, and $\epsilon_\infty = 2.34$. The Debye relaxation times and the parameters of the resonant component are $\tau_1 = 8.76$ ps, $\tau_2 = 0.224$ ps, $\omega_s/2\pi = 5.3$ THz, $\gamma_s/2\pi = 5.30$ THz, and $A_S/(2\pi)^2 = 35.1$ THz$^2$.

The parameter $f_d(\omega)$ [Eq. (9)] accounts for the difference between the external and the local directing (torque) fields. It depends on frequency through the dielectric constant. This parameter is often associated with the field within an empty cavity in a liquid [21]. An expression recently derived by us for this property [31] was used in the calculations: $f_d(\omega) = \{7[\epsilon(\omega) + 1]^2 + 8\epsilon(\omega)\}/\{12\epsilon(\omega)[2\epsilon(\omega) + 1]\}$.

Since the polarizability of many organic substances is close to $\alpha_{0,e} = \sigma_0^3/16$, the parameter of dipolar density of the solutes [Eq. (16)] was taken in the form

$$y_0(\omega) = \left\{ \frac{1}{2} + 4g_{0,\mathrm{K}}^T (m_0^*)^2 [1 - i\omega\Phi(-\omega)] \right\} \eta_0, \tag{A2}$$

where $(m_0^*)^2 = \beta\langle \mathbf{M}^2 \rangle / \sigma_0^3$ is the reduced effective dipole; $\mathbf{M}$ can be either the protein dipole or the entire dipole moment of the protein-water cluster.

Simulations of hydrated plastocyanin were reported previously [18]. The presently used data [19] represent the same simulation protocol applied to the oxidized (total charge of −8) state of plastocyanin extended to a larger number of waters in the simulation box, $N_w = 21\,076$. For plastocyanin calculations $\mathbf{M}$ represents the total dipole of the protein and water shell extending $\simeq 20$ Å from the protein surface into the bulk. This latter magnitude was added to the effective radius of the protein listed in Table I to obtain the effective

TABLE I. Solute parameters used in the calculations.

| Solute | $(\sigma_0/2)$ (Å) | $m_0$ (D) | $\tau_0$ (ns) |
|---|---|---|---|
| Trehalose | 8.2 | 1.75 | 0.05 |
| $\lambda_{6-85}$ | 12.1[a] | 61[b] | 3 |
| Plastocyanin[c] | 16.8[d] | 248[e] | 2.8[f] |

[a]From [17]. The following set of parameters from [49] was used to represent the protein-protein interaction potential in Eq. (29): $\sigma_0$ =31.8 Å, $\epsilon/k_B$=419 K, and $\delta$=4.14 Å.
[b]Calculated from equilibrated protein geometry and atomic partial charges [55].
[c]According to molecular dynamics (MD) simulation data from Ref. [18].
[d]From the vdW volume of the protein using the AMBER FF03 force field.
[e]$\langle m_0 \rangle$ calculated from the MD trajectory relative the center of mass, total charge of the Ox state of the protein is −8. Fluctuations of the protein dipole are caused by protein's vibrations.
[f]Calculated from the exponential fit of the time self-correlation function of the protein dipole.

radius of the water/protein cluster. The average squared protein/water dipole calculated from the simulation trajectory is $\langle \mathbf{M}^2 \rangle = 1.44 \times 10^6$ D$^2$. The response function $\Phi(\omega)$ was obtained as a Laplace-Fourier transform of the three-exponent fit of the simulated correlation function,

$$\Phi(t) = \sum_{i=1}^{3} A_i e^{-t/\tau_i}, \tag{A3}$$

where $A_i = \{0.84, 0.11, 0.05\}$ and $\tau_i = \{0.14, 1790, 6.3\}$ ps.

Other solute parameters used in the calculations are listed in Table I. The hard-sphere diameter of water was taken at the value of $\sigma$=2.87 Å and the inertial parameter $p'$ in Eq. (20) was set at the value of $p'$=0.1 [28]. The rotational relaxation times of the solutes were taken at $\tau_0$=50 ps for trehalose and $\tau_0 \simeq 3$ ns for the two proteins. The former number is consistent with the second relaxation process extracted from the dielectric response and simulations of hydrated saccharides [52], while the latter is typical for rotational dynamics of proteins [42].

The calculation of the solute dipole component of the dielectric response simplifies in the continuum limit when the integral in Eq. (18) loses the dependence on frequency and reduces to Eq. (21). This integral depends on two parameters, the volume fraction $\eta_0$ and the reduced geometry parameter $r = 1/2 + \sigma/(2\sigma_0)$, when the hard-spheres approximation is used for the density structure factor $S_0(k, \eta_0)$. The range $0.5 \le r \le 1$ covers most problems of interest. Numerical integration of Eq. (21) with the PY density structure factor [26] was done in this range of $r$-values and volume fractions in the range $0 \le \eta_0 \le 0.3$. The numerical results were interpolated with the polynomial function

$$I(\eta_0, r) = a(\eta_0) + b(\eta_0) r^2 + c(\eta_0) r^4 + d(\eta_0) r^6, \tag{A4}$$

where

$$a(\eta_0) = 1 + 0.225\,\eta_0 + 7.726\,\eta_0^2 - 13.805\,\eta_0^3,$$

$$b(\eta_0) = -9.694\,\eta_0 - 18.572\,\eta_0^2 + 16.642\,\eta_0^3,$$

$$c(\eta_0) = 6.987\,\eta_0 + 38.913\,\eta_0^2 - 5.940\,\eta_0^3,$$

$$d(\eta_0) = 2.108\,\eta_0 - 16.570\,\eta_0^2 - 10.007\,\eta_0^3. \tag{A5}$$

The expansion in even powers of $r$ in Eq. (A4) is dictated by the symmetry of the density structure factor [26] and the density expansion of the polynomial coefficients has been chosen to justify the ideal-solution limit $I(0, r) = 1$.


[1] B. K. P. Scaife, *Principles of Dilectrics* (Clarendon Press, Oxford, 1998).
[2] T. C. Choi, *Effective Medium Theory* (Clarendon Press, Oxford, 1999).
[3] S. Takashima, *Electrical Properties of Biopolymers and Membranes* (Adam Hilger, Bristol, 1989).
[4] M. C. Beard, G. M. Turner, and C. A. Schmuttenmaer, J. Phys. Chem. B **106**, 7146 (2002).
[5] K. Yokoyama, T. Kamei, H. Minami, and M. Suzuki, J. Phys. Chem. B **105**, 12622 (2001).
[6] A. Bergner, U. Heugen, E. Bründermann, G. Schwaab, M. Havenith, D. R. Chamberlin, and E. E. Haller, Rev. Sci. Instrum. **76**, 063110 (2005).
[7] J. R. Knab, J.-Y. Chen, Y. He, and A. G. Markelz, Proc. IEEE **95**, 1605 (2007).
[8] H. Frauenfelder, G. Chen, J. Berendzen, P. W. Fenimore, H. Jansson, B. H. McMahon, I. R. Stroe, J. Swenson, and R. D. Young, Proc. Natl. Acad. Sci. U.S.A. **106**, 5129 (2009).
[9] S. Ebbinghaus, S. J. Kim, M. Heyden, X. Yu, M. Gruebele, D. M. Leitner, and M. Havenith, J. Am. Chem. Soc. **130**, 2374 (2008).
[10] C. Zhang and S. M. Durbin, J. Phys. Chem. B **110**, 23607 (2006).
[11] J. Xu, K. W. Plaxco, and S. J. Allen, Protein Sci. **15**, 1175 (2006).
[12] J. B. Baxter and C. A. Schmuttenmaer, J. Phys. Chem. B **110**, 25229 (2006).
[13] M. Alcoutlabi and G. B. McKenna, J. Phys.: Condens. Matter **17**, R461 (2005).
[14] D. V. Matyushov, J. Chem. Phys. **120**, 1375 (2004).
[15] D. N. LeBard and D. V. Matyushov, J. Chem. Phys. **128**, 155106 (2008).
[16] M. Heyden, E. Bründermann, U. Heugen, D. M. Leitner, and M. Havenith, J. Am. Chem. Soc. **130**, 5773 (2008).
[17] S. Ebbinghaus, S. J. Kim, M. Heyden, X. Yu, U. Heugen, M. Gruebele, D. M. Leitner, and M. Havenith, Proc. Natl. Acad. Sci. U.S.A. **104**, 20749 (2007).
[18] D. N. LeBard and D. V. Matyushov, Phys. Rev. E **78**, 061901

(2008).
[19] D. N. LeBard and D. V. Matyushov, J. Phys. Chem. B (to be published).
[20] L. D. Landau and E. M. Lifshitz, *Electrodynamics of Continuous Media* (Pergamon, Oxford, 1984).
[21] C. J. F. Böttcher, *Theory of Electric Polarization* (Elsevier, Amsterdam, 1973), Vol. 1.
[22] P. Madden and D. Kivelson, Adv. Chem. Phys. **56**, 467 (1984).
[23] M. Neumann, Mol. Phys. **57**, 97 (1986).
[24] D. F. Plusquellic, K. Siegrist, E. J. Heilweil, and O. Esenturk, ChemPhysChem **8**, 2412 (2007).
[25] D. Chandler, Phys. Rev. E **48**, 2898 (1993).
[26] J. P. Hansen and I. R. McDonald, *Theory of Simple Liquids* (Academic Press, Amsterdam, 2003).
[27] M. S. Wertheim, J. Chem. Phys. **55**, 4291 (1971).
[28] D. V. Matyushov, J. Chem. Phys. **122**, 044502 (2005).
[29] G. Stell, G. N. Patey, and J. S. Høye, Adv. Chem. Phys. **48**, 183 (1981).
[30] L. Onsager, J. Am. Chem. Soc. **58**, 1486 (1936).
[31] D. R. Martin and D. V. Matyushov, Europhys. Lett. **82**, 16003 (2008).
[32] J. G. Kirkwood and F. B. Buff, J. Chem. Phys. **19**, 774 (1951).
[33] L. Belloni, J. Phys.: Condens. Matter **12**, R549 (2000).
[34] D. V. Matyushov, J. Chem. Phys. **120**, 7532 (2004).
[35] B. Bagchi and A. Chandra, Adv. Chem. Phys. **80**, 1 (1991).
[36] T. Kihara and K. Miyoshi, J. Stat. Phys. **13**, 337 (1975).
[37] C. Barrio and J. R. Solana, Mol. Phys. **97**, 797 (1999).
[38] L. Zhang, L. Wang, Y.-T. Kao, W. Qiu, Y. Yang, O. Okobiah, and D. Zhong, Proc. Natl. Acad. Sci. U.S.A. **104**, 18461 (2007).
[39] A. Shukla, E. Mylonas, E. D. Cola, S. Finet, P. Timmins, T. Narayanan, and D. I. Svergun, Proc. Natl. Acad. Sci. U.S.A. **105**, 5075 (2008).
[40] Y. Liu, W.-R. Chen, and S.-H. Chen, J. Chem. Phys. **122**, 044507 (2005).
[41] C. A. Croxton, *Introduction to Liquid State Physics* (Wiley, New York, 1975).
[42] T. Rudas, C. Schröder, S. Boresch, and O. Steinhauser, J. Chem. Phys. **124**, 234908 (2006).
[43] C. H. Wang, *Spectroscopy of Condensed Media. Dynamics of Molecular Interactions* (Acedemic Press, Orlando, 1985), there is a typo in Eq. (1.175) in the book, the dielectric constant $\epsilon'(\omega)$ should be under square root, as in Eq. (26).
[44] D. A. McQuarrie, *Statistical Mechanics* (University Science Books, Sausalito, CA, 2000).
[45] H. Yada, M. Nagai, and K. Tanaka, Chem. Phys. Lett. **473**, 279 (2009).
[46] A. Gharsallaoui, B. Rogé, J. Génotelle, and M. Mathlouthi, Food Chem. **106**, 1443 (2008).
[47] W. Y. Yang and M. Gruebele, Nature (London) **423**, 193 (2003).
[48] F. Zhang, M. W. A. Skoda, R. M. J. Jacobs, R. A. Martin, C. M. Martin, and F. Schreiber, J. Phys. Chem. B **111**, 251 (2007).
[49] S. J. Kim, C. Dumont, and M. Gruebele, Biophys. J. **94**, 4924 (2008).
[50] N. Javid, K. Voggt, C. Krywka, M. Tolan, and R. Winter, ChemPhysChem **8**, 679 (2007).
[51] L. M. Xu, S. V. Buldyrev, C. A. Angell, and H. E. Stanley, Phys. Rev. E **74**, 031108 (2006).
[52] H. Weingärtner, A. Knocks, S. Boresch, P. Höchtl, and O. Steinhauser, J. Chem. Phys. **115**, 1463 (2001).
[53] S. L. Lee, P. G. Debenedetti, and J. R. Errington, J. Chem. Phys. **122**, 204511 (2005).
[54] M. Paolantoni, L. Comez, M. E. Gallina, P. Sassi, F. Scarponi, D. Fioretto, and A. Morresi, J. Phys. Chem. B **113**, 7874 (2009).
[55] D. M. Leitner (private communication).